Available online at www.sciencedirect.com
SCIENCE DIRECT®
Talanta 64 (2004) 355–360
Talanta
www.elsevier.com/locate/talanta

Human serum albumen enhanced resonance light scattering of dyes

Jia Runping, Zhai Honglin, Shen Yan, Chen Xingguo*, Hu Zhide

College of Chemistry & Chemical Engineering, Lanzhou University, Lanzhou 730000, PR China

Received 25 November 2003; received in revised form 23 February 2004; accepted 23 February 2004

Available online 10 May 2004

Abstract

For the first time, the relationship between the structural parameters of dye molecule and the enhanced resonance light scattering (RLS) of dye–human serum albumen (HSA) was investigated using chemometrics technique. The data set of the enhanced RLS intensity of the dye–HSA was obtained under the same experimental conditions for 22 dyes. After calculated with HyperChem software and selected by stepwise regression approach, six structural parameters for the maximum RLS wavelength were used in multivariable linear regression (MLR) ($R = 0.932$), seven structural parameters for the corresponding enhanced RLS intensity were employed by MLR ($R = 0.934$). According to these models, the maximum RLS wavelength and the enhanced RLS intensity are both attributed to the spatial structure and energies of dye.

Keywords: Dye structure; Human serum albumen; Resonance light scattering; Chemometrics technique

1. Introduction

Resonance light scattering (RLS) is an effective technique for studying the aggregation of dyes and the aggregates, as well as the structures of various complexes and macromolecules [1–3]. Because all of the absorption processes are inherently associated with light scattering, all kinds of dyes have their own RLS spectra. It is possible to enhance the weak resonance light scattering of small dye molecule through their binding with macromolecules, such as nucleic acids and proteins. Pasternack et al. [3], developed a technique to detect the RLS by using a common spectrofluorimeter that simplifies the detection process and confers on this technique not only high sensitivity and good selectivity but also simplification. In this contribution, Huang first used RLS for analytical purpose to determine the quantities of nucleic acids with tetrakis (4-trimethylammoniumphenyl) porphyrin (TAPP) [4]. Based on this, numerous sensitive methods for the determination of macromolecules have been developed in the available literature [5–8]. However, the relationship between the structure of small dye and the RLS response of dye–human serum albumen (HSA) is not well known. In this paper, the relationship between the structure of small dye and the RLS spectra of dye–HSA was investigated for the first time. We found that the appearance of RLS band and the enhancing RLS phenomena of dye–HSA were both attributed to the spatial configuration and energies of dye molecule.

2. Experimental

2.1. Apparatus

The resonance light scattering spectra of all the samples were measured at room temperature by a Hitachi M-850 fluorescence spectrophotometer with a Xe lamp as the excitation light source. A model pHS 10A pH meter (Xiaoshan, China) was used to measure the acidity of the tested solutions.

2.2. Reagents

All dyes were directly dissolved in water to prepare a stock solution of 1000 μmol l^{-1}. More dilute solutions were prepared as required. HSA (from Sigma, St. Louis, MO) was directly dissolved in doubly distilled water to prepare a stock solution of 1000 μg ml^{-1}, which was kept at 0–4 °C. Working solutions with lower concentrations were freshly prepared by appropriate dilution of the stock solution with

* Corresponding author. Tel.: +86-931-8912540; fax: +86-931-8912582.
E-mail addresses: chenxg@lzu.edu.cn, jrpchem@vip.sina.com (C. Xingguo).

0039-9140/$ – see front matter © 2004 Elsevier B.V. All rights reserved.
doi:10.1016/j.talanta.2004.02.030

water prior to use. A pH 4.1 of Britton–Robbinson (BR) solutions (composed of 0.04 mol l^{-1} H_3PO_4, 0.04 mol l^{-1} HOAc, 0.04 mol l^{-1} H_3BO_3 and an appropriate concentration of NaOH) were used to control the acidity of the aqueous system. All other chemicals were of analytical or the best grades commercially available and doubly distilled water was used throughout.

2.3. General procedures

The procedure started by placing 1.0 ml of pH 4.1 BR buffer in a 10 ml flask, adding 1.0 ml of 250 μmol l^{-1} dye and mixing. Then 2.0 ml of 100 μg ml^{-1} HSA was added and mixed. This was made up to volume with water and mixed thoroughly. Then the RLS intensity was measured by scanning synchronously with the same excitation and emission wavelengths ($\Delta\lambda = 0.0$ nm) through the wavelength range of 380–430 nm, against a reagent blank prepared in a similar way, but without HSA. Here, the RLS spectra of two dyes and corresponding dye–HSA mixtures as representative spectra were presented in Fig. 1.

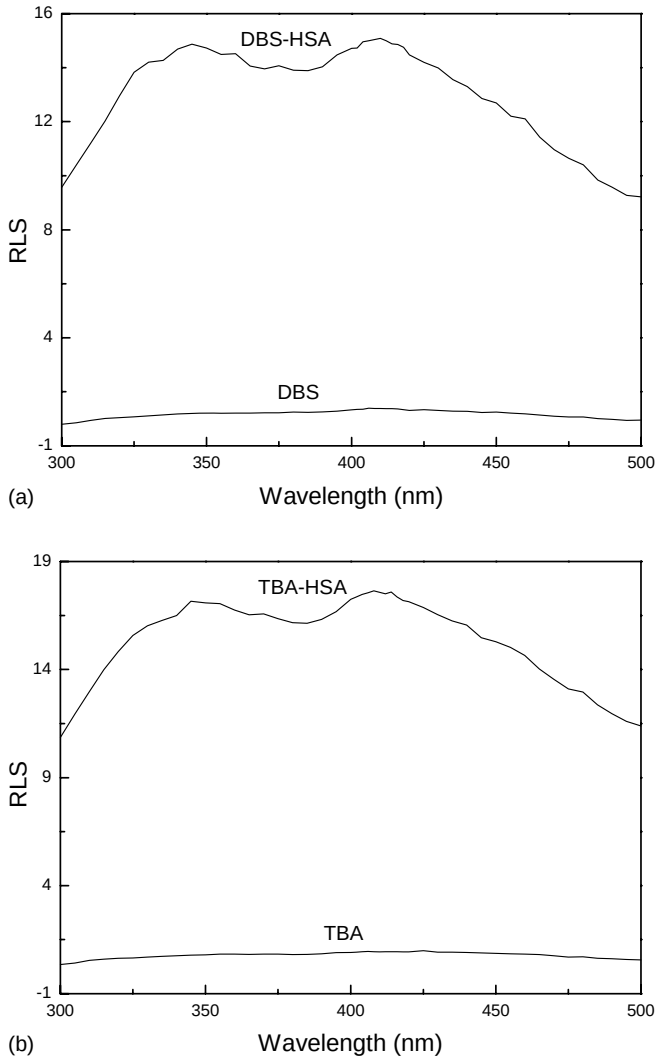

Fig. 1. RLS spectra of (a) Arsenazo-DBS (DBS) and (b) Tribromoarsenazo (TBA). Concentrations: dye 25.0 μmol l^{-1}, HSA 20.0 μg ml^{-1}, pH 4.1, and $\lambda_{ex} = \lambda_{em}$.

3. Data and methods

3.1. Data set

From Fig. 1, it was clear that the RLS intensity of dye was very small and nearly constant. However, when HSA was added, an obvious RLS band of dye–HSA appeared and the maximum peak was located at 410 nm. Additionally, the RLS intensity of dye–HSA was much higher than that of dye alone due to the formation of the aggregates of dye–HSA. Therefore, the data used in this research were given as the enhanced RLS intensity, which was the RLS difference between dye and dye–HSA under the same experimental conditions, and corresponding wavelength was the maximum RLS wavelength. The data set is presented in Table 1. To avoid unreal variations due to different units and/or scalar levels, the data set were standardized by the expressions as follows.

$$x_{ij}^{*} = \frac{x_{ij} - \bar{x}_j}{s_j}, \qquad \bar{x}_j = \frac{1}{n}\sum_{i=1}^{n} x_{ij},$$

$$s_j^2 = \frac{1}{n-1}\sum_{i=1}^{n}(x_{ij} - \bar{x}_j)^2, \quad n = 22$$

So, for the every variable, the mean equals 0 and variance is 1.

Table 1
The dye structure and enhanced intensity of dye–HSA[a]

Number	Dye structure	Wavelength (nm)	RLS intensity
1	Acidic chrome blue K	410.0	5.209
2	Eriochrome blue black R	407.7	9.405
3	Berryllon II	409.9	12.686
4	Kalces Salt	405.5	11.786
5	Arsenazo-DBS	409.0	13.696
6	Tribromoarsenazo	408.6	16.698
7	Chlorophosphonazo-pB	408.6	5.354
8	Arsenazo-DBN	409.6	11.745
9	Chlorophosphonazo-DBOK	408.4	17.621
10	Chlorophosphonazo-mA	408.5	15.513
11	Chlorophosphonazo-DBM	408.2	12.741
12	p-Idochlorophosphonazo	408.2	11.985
13	Erichrome black T	408.6	4.676
14	Cal-Red	407.7	11.242
15	Arsenazo-DBC	409.2	10.429
16	Arsenazo-DBM	409.5	11.823
17	Congo red	399.7	2.076
18	Arsenazo I	405.0	14.205
19	Arsenazo II	409.5	1.4
20	Sulfonazo	406.2	11.355
21	Fuchsine	409.2	1.119
22	Chlorophosphonazo-mk	408.5	13.172

[a] Concentrations: dye 25.0 μmol l^{-1}, HSA 20.0 μmol l^{-1}, pH 4.1, and $\lambda_{ex} = \lambda_{em}$.

3.2. Software and hardware

With development and application of computer technology, a lot of complex calculation and plotting can be finished easily by using these modeling tools, such as Matlab, ChemOffice, SPSS, etc. The structural parameters were calculated by HyperChem software, stepwise regression technique was employed to select parameters. All of these works was completed with PC (PII 350 MHz/128M).

4. Results and discussion

4.1. Calculations of structural parameters

To obtain a QSPR model, compounds are often represented using molecular descriptors. The calculation process of the molecular descriptors is described as below. All molecular structures of 22 dyes were drawn into HyperChem and pre-optimized using MM+ molecular mechanics force field. A more precise optimization was done with semi-empirical PM3 method utilizing the Polak–Ribiere algorithm until the root mean square gradient arrived 0.001 in HyperChem. All calculations were carried out at restricted Hartree Fock level with no configuration interaction. Then 14 quantum structural parameters were obtained. The Wiener index and Balaban index of dye molecules could be calculated [9,10]. The parameters used and all of the results calculated are shown in Table 2.

4.2. Selection of structural parameters and modeling

The calculated structural descriptors and the experimental results were analyzed using SPSS (version 10.0) software. To select the significant structural descriptors, the stepwise regression was performed, which form is as follows: $I = b_0 + b_1D_1 + b_2D_2 + \cdots + b_nD_n$, where I is dependent variable, D_1, D_2 and D_n are the descriptors, the intercept (b_0) and the regression coefficients of the descriptors ($b_1, b_2, \ldots, b_n$) are determined by using the least squares method and n is the number of the descriptors. In order to evaluate the proposed model, the correlation coefficient (R), its standard error, F-value have been considered [11]. The maximum RLS wavelength and RLS intensity were considered as a dependent variable, respectively. The structural parameters were considered as independent variables, and so two regression equations were obtained by stepwise regression analysis for standardized data set as follows:

The model-1 for the maximum RLS wavelength:

$$Y_w = -3.131\text{BE} - 0.465\text{HOMO} + 1.340\text{volume} - 0.435\text{HE} - 11.562\text{WI} + 7.130\text{BI}$$
$$(R = 0.932,\ F = 16.66,\ \text{and}\ P = 0.000)$$

The model-2 for the enhanced RLS intensity:

$$Y_I = 2.959\text{TE} + 0.504\text{HOMO} + 4.886\text{mass} - 0.647\log P + 1.069\text{HE} - 4.872\text{polar} + 3.445\text{RI}$$
$$(R = 0.934,\ F = 13.56,\ \text{and}\ P = 0.000)$$

The detailed results of the regressions were presented in Tables 3–5. The F-test of the regression equations and the T-test of the regression coefficients indicated that the conclusion of stepwise regression analysis was reliable in the statistical sense. According to the above stepwise models, the predicted and observed results for the maximum RLS wavelength and the enhanced RLS intensity are presented in Figs. 2 and 3.

4.3. Discussion of the stepwise regression models

4.3.1. Effect of structural parameters on RLS wavelength

Based on our previous studies [6–9,12–15], we found that the RLS response is different by fixing the other same experimental conditions only choosing different detection probe (dye), so dye structure should have some effect on the RLS wavelength. To better guide the experiment, the relationship between dye structure and the RLS wavelength was investigated, and a regression model using the stepwise regression method was established (see model-1). From the model-1, it was clear that these structural parameters, binding energy (BE), HOMO, volume, hydration energy (HE), Wiener index (WI), and Balaban index (BI), were involved. Wiener index expresses the compactness of molecule, Balaban index reflects the degree of embranchment in molecule, binding energy and hydration energy both reflects the steady instance of molecule, HOMO represents the reactive power of molecule, and volume directly reflects the size of molecule. According to the regression coefficients of the model-1, it was seen that Wiener index, Balaban index, and binding energy were mainly responsible for the maximum RLS wavelength. Here, Wiener index and Balaban index both reflect the spatial configuration of dye, while the binding energy, hydration energy and HOMO represent the energy state of dye molecule. In our opinion, the energy state of dye molecule indirectly affected its spatial configuration in a solution, which in turn affected the size of the dye–HSA aggregate. Thus, the spatial configuration of dye was an important factor that affected the maximum RLS wavelength. The small coefficient of HOMO in the model-1 demonstrated that the interaction between the dye and HSA was not due to chemical bond but mainly intermolecular force, such as electrostatic attraction, hydrophobic force, Van der Waals force, etc. may be involved.

4.3.2. Effect of structural parameters on RLS intensity

It was reported earlier [1,12] that the intensity of the enhanced RLS signal appeared to depend on the electronic properties of the individual chromophores, the extent of electronic coupling among chromophores and the size of

Table 2
The structural parameters calculated (standardized)

Number	QM	BE	TE	EE	Heat	DM	HOMO	LUMO	Mass	Volume	log *P*	HE	Polar	RI	WI	BI	HSA-1	HSA-2
1	−0.1296	1.2787	1.4347	1.3365	0.8610	−0.1410	−1.7979	0.5089	−1.4850	−1.3779	0.7327	0.5745	−1.5610	−1.5263	−1.0347	−0.8096	0.8963	−1.0437
2	−0.1090	1.0883	1.3285	1.2074	1.1556	0.3326	1.1677	0.6463	−1.3507	−1.3534	0.9217	0.4226	−1.2254	−1.1973	−0.9676	−0.8149	−0.1183	−0.1783
3	−0.3438	0.1865	−0.2652	−0.0713	−1.0458	−0.6029	−0.5108	0.7602	−0.1637	−0.1001	−0.6694	−0.6949	−0.6636	−0.1293	−0.1945	−0.2638	0.8522	0.4983
4	−0.0780	0.8074	1.0065	0.9606	0.6912	−0.8573	−0.2173	−0.5042	−1.1468	−1.1416	0.6358	1.8498	−0.9928	−1.0487	−0.8432	−0.7502	−1.0888	0.3127
5	−0.3398	−0.2107	−0.6885	−0.5220	−0.5765	0.3824	−0.0667	−0.5042	0.9469	0.6160	0.0870	−0.8772	0.4882	0.5073	0.2836	0.2330	0.4552	0.7066
6	−0.1929	0.0899	−0.3560	−0.2189	0.1284	−0.2805	−1.0227	−0.1233	0.9415	0.3551	0.4836	−0.4640	0.5602	0.3513	−0.0303	−0.0999	0.2787	1.3256
7	−0.0554	0.0076	−0.1843	−0.0849	−0.2950	−0.8837	−0.3829	0.0455	0.1664	0.2015	0.3314	−0.4434	0.0723	0.2643	−0.0988	−0.1770	0.2787	−1.0138
8	−0.0581	−0.0727	−0.5352	−0.3849	0.0624	0.2775	−1.0979	−2.6953	0.7845	0.4265	−1.6978	−0.6894	0.4882	0.2938	0.1670	0.1075	0.7199	0.3042
9	−0.1802	−0.2485	−0.6603	−0.4960	−0.7121	−0.6967	−0.9474	−1.3092	0.7359	0.5414	0.0732	1.0112	0.5447	0.5995	0.2631	0.2195	0.1905	1.5160
10	−0.0599	−0.1783	−0.4066	−0.3312	−0.2906	0.5231	0.0387	−0.1312	0.5969	0.4225	0.4283	−0.4093	0.4791	0.5569	0.0580	−0.0057	0.2346	1.0813
11	−0.2949	−0.4271	−0.2863	−0.2684	−0.5672	1.9105	0.1892	−0.0173	−0.0044	0.3461	0.2761	1.2554	0.1754	0.3141	0.0805	0.0082	0.1023	0.5096
12	−0.3055	0.0172	−0.1548	−0.0727	−0.2329	−0.2149	0.0763	−0.0330	0.3841	0.2656	0.5482	−0.4596	0.2912	0.3827	−0.0988	−0.1770	0.1023	0.3537
13	−0.0037	0.9468	0.9950	0.9640	1.1051	2.9369	−1.6474	−0.6456	−1.1422	−1.1648	−1.2366	0.2603	−1.0576	−1.0680	−0.8370	−0.7484	0.2787	−1.1536
14	−0.1008	0.8047	1.0065	0.9603	0.6770	−0.6264	0.4376	−0.0369	−1.1468	−1.1385	0.6358	1.9189	−0.9928	−1.0487	−0.8432	−0.7502	−0.1183	0.2005
15	−0.0899	0.0790	−0.3393	−0.2144	0.0622	−0.5965	−0.1947	−0.4650	0.7356	0.3315	0.3545	−0.5082	0.4964	0.2816	−0.0303	−0.0999	0.5434	0.0328
16	−0.0111	−0.1467	−0.2701	−0.2130	0.0417	−0.0191	0.1215	0.0298	0.6410	0.3504	0.5390	−0.4646	0.4873	0.2707	−0.0303	−0.0999	0.6758	0.3203
17	−0.1654	−1.2236	0.0964	0.0469	1.4477	−0.7348	2.3194	0.3989	−0.1539	0.6436	0.3591	−0.2432	1.0226	0.9153	0.6665	0.0565	−3.6475	−1.6898
18	−0.1223	1.0530	0.6054	0.7270	−0.3753	0.1474	0.8064	2.0246	−0.6375	−0.8889	0.2392	−0.3280	−1.2272	−1.1757	−0.7701	−0.6688	−1.3094	0.8115
19	−0.3492	−2.5063	−2.1831	−2.5290	−2.3568	1.1380	1.6269	1.0861	1.8937	2.0960	−1.2366	−1.9695	2.1325	1.8431	2.8302	3.1822	0.6758	−1.8292
20	−1.2741	−2.2636	−1.7647	−2.1115	−1.1057	−1.1064	0.2193	−0.8655	1.1812	1.8864	−3.0629	−1.4652	1.6947	2.0009	2.4993	2.5251	−0.7800	0.2238
21	4.3200	1.2192	1.9733	1.5868	2.1405	−1.2758	1.0247	1.8440	−1.7816	−1.5690	1.2307	0.7027	−1.2783	−1.6137	−1.1502	−0.8749	0.5434	−1.8871
22	−0.0564	−0.3007	−0.3522	−0.2714	−0.8147	0.3877	−0.1420	−0.0134	0.0048	0.2517	0.0270	1.0210	0.0660	0.2262	0.0805	0.0082	0.2346	0.5985

QM: maximum negative charge; BE: binding energy; TE: total energy; EE: electronic energy; heat: heat of formation; DM: dipole moment; HOMO: energy of highest occupied molecular orbital; LUMO: energy of lowest unoccupied molecular orbital; mass: molecular mass; volume: molecular volume; log *P*: the octanol/water partition coefficient; HE: hydration energy; WI: Wiener index; BI: Balaban index; polar: polarizability; RI: refractive index.

Table 3
The results selected of the parameters by stepwise regression

Item	The parameters selected	S.D.
Wavelength	BE, HOMO, volume, HE, EE, WI	0.345
RLS intensity	TE, HOMO, mass, log *P*, HE, polar, RI	0.343

Table 4
The results of the maximum RLS wavelength by stepwise regression

Variables	Coefficients	S.D.	*t*	*P*-value
Constant	4.513E−15	0.091	0.000	1.000
BE	−3.131	1.143	−2.739	0.015
HOMO	−0.465	0.129	−3.613	0.003
Volume	1.340	0.414	3.236	0.006
HE	−0.435	0.178	−2.450	0.027
WI	−11.562	2.042	−5.663	0.000
BI	7.130	1.049	6.796	0.000

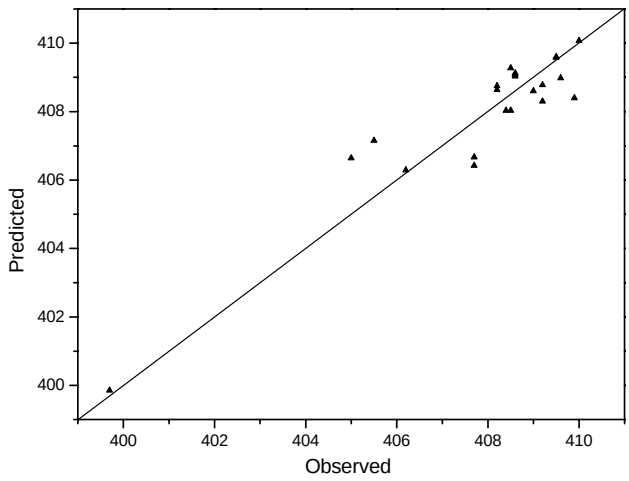

Fig. 2. Predicted vs. observed for RLS wavelength (nm).

the aggregate formed. Based on the model-2 established in this study, we found that the enhanced RLS intensity of dye–HSA is correlative with the structure and energies of dye molecule, which may be attributed to an extended array of electronically coupled chromophores with large oscillator strength. The influence of dye structure on the RLS intensity may be explained as the effect of this array extended, which was supported by larger coefficients of polarizability (polar), refractivity index (RI), and mass in the model-2. Polarizability represents the polarizable capacity of molecule, refractivity index is a combined measure of its size and polarizability, mass indirectly reflects the size of molecule, and log *P* is the hydrophobic index of molecule. These four structure parameters, mass, polar, RI and log *P*, reflect the size and distortional power of dye molecule together, which are two important factors that affects the electronic delocalization, thus, the RLS intensity was affected. Of course, the formation of the dye–HSA aggregate was closely relative with the molecular information of HSA. Both total energy and hydration energy that reflect the energy levels of dye molecule affected the RLS intensity, as shown in the model-2. Moreover, HOMO with small coefficient indicated that the influence of HOMO on the RLS intensity was small. Based on above discussion, we inferred that the enhancing RLS intensity was relative with not only the state of dye molecule but also the spatial configuration of HSA.

Table 5
The results of the RLS intensity by stepwise regression

Variables	Coefficients	S.D.	*t*	*P*-value
Constant	1.738E−14	0.094	0.000	1.000
TE	2.959	0.768	3.855	0.002
HOMO	0.504	0.165	3.052	0.009
Mass	4.886	0.755	6.469	0.000
log *P*	−0.647	0.212	−3.053	0.009
HE	1.069	0.176	6.084	0.000
Polar	−4.872	0.757	−6.433	0.000
RI	3.445	0.774	4.450	0.001

As we know, the structure of HSA is described as being composed of three homologous domains linked together by peptide chains. Almost all the hydrophobic amine acid residues are placed between the 'helices' and inside the trough, whereas the great majority of polar residues are on the outer wall of the structure. So the cylindrical domain has a hydrophobic interior and a polar exterior [16]. In a pH 4.1 solution, the tight conformation of HSA can be readily converted to the highly charged unfolded state. As a result, almost all hydrophobic groups of HSA molecule in a dispersed state unfolds, the HSA molecules with an expandable form can accept a larger number of protons than the same well-known HSA. Being driven by hydrophobic force caused by the non-polar sidechain in the polypeptide chain of HSA, a hydrophobic nucleus is formed; whose surface distributes numerous charged sidechain. HSA is positive charged when the acidity of solution is lower than the isoelectronic point (pI = 4.8), so there must be a lot of binding sites. From the structures of all probe dye selected

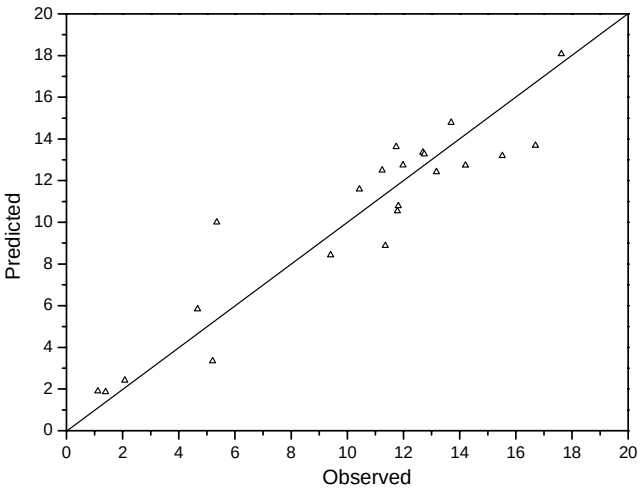

Fig. 3. Predicted vs. observed for RLS intensity.

in this study, it was clear that these probe molecules have charged hydrophilic groups, such as hydroxy and sulfonic acid group. Moreover, they also have non-charged hydrophobic groups, such as phenyl nucleus and other aromaticity nucleus. When the negative dye probe was absorbed on the surface of HSA, dye binds to protonated amine groups of amino acid residues in the polypeptide chain to form the dye–HSA complex due to the electrostatic attraction. Meanwhile, the aggregation was stabilized through the combination of hydrophobic groups of dye molecule and hydrophobic amine acid residues, and this stimulated the electronic delocalization of the dye–HSA aggregate. Thus, an evident RLS enhancing response was observed (see Fig. 1), which was consistent with the regression model established in this study. Moreover, our conclusion was in accordance with previous reports.

5. Conclusion

In this study, the relationship between the molecular structure of dye and the enhanced RLS of dye–HSA was investigated by chemometrics approach, and two models with satisfactory accuracy were developed for the experimental data set and the structural descriptors selected. In our opinions, the spatial configuration and the energy levels of dye molecule were mainly responsible for the RLS wavelength of dye–HSA, while the enhanced RLS intensity of dye–HSA was attributed to the state of dye molecule and the spatial configuration of HSA. Moreover, the aggregation of dye on the surface of HSA was due to intermolecular force mainly, not chemical bond. Based on the above two models, we believe that they may help us find other new spectral probes for the HSA determination.

References

[1] R.F. Pasternack, P.J. Collings, Science 269 (1995) 935.
[2] J. Anglister, I.Z. Steinberg, Chem. Phys. Lett. 65 (1979) 50.
[3] R.F. Pasternack, C. Bustamante, P.J. Collings, A. Giannetto, E.J. Gibbs, J. Am. Chem. Soc. 115 (1993) 5393.
[4] C.Z. Huang, K.A. Li, S.Y. Tong, Anal. Chem. 68 (1996) 2259.
[5] S.P. Liu, H.Q. Luo, N.B. Li, Z.F. Liu, W.X. Zheng, Anal. Chem. 73 (2001) 3907.
[6] Q.F. Li, H.Y. Zhang, C.X. Xue, X.G. Chen, Z.D. Hu, Spectrochim. Acta, Part A 56 (2000) 2465.
[7] Q.F. Li, X.G. Chen, H.Y. Zhang, C.X. Xue, S.H. Liu, Z.D. Hu, Analyst 125 (2000) 1483.
[8] L.J. Dong, R.P. Jia, Q.F. Li, X.G. Chen, Z.D. Hu, Fresenius J. Anal. Chem. 370 (2001) 1009.
[9] H. Wiener, J. Am. Chem. Soc. 69 (1947) 17.
[10] A.T. Balaban, J. Chem. Inf. Comput. Sci. 25 (1985) 334.
[11] L. Xu, Methods of Chemometrics, Science Press, Beijing, 1997, p. 53.
[12] R.P. Jia, L.J. Dong, Q.F. Li, X.G. Chen, Z.D. Hu, Talanta 57 (2002) 693.
[13] R.P. Jia, L.J. Dong, Q.F. Li, X.G. Chen, Z.D. Hu, Anal. Chim. Acta 30 (2001) 2333.
[14] L.J. Dong, R.P. Jia, Q.F. Li, X.G. Chen, Z.D. Hu, Analyst 126 (2001) 707.
[15] Q.F. Li, L.J. Dong, R.P. Jia, X.G. Chen, Z.D. Hu, Spectrosc. Lett. 34 (2001) 407.
[16] K.H. Ulrich, Pharmacol. Rev. 33 (1981) 17.